

---

REVIEW

---

## Dielectric and Photoelectric Properties of Photosynthetic Reaction Centers

C. S. Chamorovsky<sup>1</sup>, S. K. Chamorovsky<sup>2</sup>, and A. Yu. Semenov<sup>1\*</sup>

<sup>1</sup>Belozersky Institute of Physico-Chemical Biology and <sup>2</sup>Department of Biophysics, Faculty of Biology, Lomonosov Moscow State University, Moscow, Russia; fax: (7-095) 939-3181; E-mail: semenov@genebee.msu.su

Received July 27, 2004

**Abstract**—A brief review of studies of dielectric and photoelectric properties of photosynthetic reaction centers of purple bacteria as well as photosystem I and photosystem II of cyanobacteria and higher plants is given. A simple kinetic model of the primary processes of electron transfer in photosynthesis is used to discuss possible mechanisms of correlation between rate constant of charge transfer reaction, free energy of electron transition, and effective dielectric constant in the locus of corresponding carriers.

**Key words:** photosynthetic reaction center complexes, photosynthetic bacteria, photosystems I and II, cyanobacteria, electron transfer, membrane potential, dielectric constant

The processes of charge separation in photosynthetic reaction centers (RC) and further transfer of electron and proton along the photosynthetic chain are accompanied by generation of electric potential ( $\Delta\psi$ ), which can be detected using instrumental methods. The direct electrometric method suggested in our laboratory at the Belozersky Institute of Physico-Chemical Biology provided the opportunity to detect the rise-time of  $\Delta\psi$  within the range from 200 nsec to 100 msec [1]. This method was used to study bacteriorhodopsin [2], bacterial photosynthetic reaction centers (BRC) [3], as well as photosystem (PS) I [4, 5] and PS II [6] of cyanobacteria.

Because the photoelectric signal amplitude measured by this method is proportional to dielectrically weighted distances, comparison of projections of the distance vectors between redox cofactors onto the membrane normal with the relative photovoltage amplitudes provides an opportunity to estimate the dielectric constant value ( $\epsilon$ ) at the corresponding chain segment.

Strictly speaking, dielectric constant is a macroscopic characteristic determined by the atomic state of the surrounding medium. This value can be calculated from the classical equation of electrostatics:

$$E_e = \frac{1}{4\pi\epsilon_0} \frac{e}{R^2} \mathbf{r}, \quad (1)$$

where  $E_e$  is the strength of the electric field generated by an electron at the locus of a given atom in vacuum;  $\epsilon_0$  is the dielectric permittivity of vacuum;  $e$  is electron charge;  $\mathbf{r}$  is unity radius-vector connecting atom and electron;  $R$  is the distance between the atom and the electron.

Local (i.e., determined on the time scale of corresponding reaction) value of dielectric constant ( $\epsilon_{\text{eff}}$ ) can be calculated from Eq. (2) derived in [7, 8]:

$$\epsilon_{\text{eff}} = \frac{E_e}{E_{\text{net}}}, \quad (2)$$

where  $E_{\text{net}}$  is the net electric field strength at the chromophore locus with regard to the effect of charge screening.

It was demonstrated in various model systems, including genetically modified proteins (for example, barnase) that the macroscopic estimates of dielectric parameters did not change drastically on the angstrom scale [9, 10].

Photoelectric and dielectric properties of PS I were considered in our earlier reviews [11, 12]. The goal of this work was to review photoelectric and dielectric properties of BRC and PS II and to discuss possible mechanisms of correlation between values of charge transfer reaction rate constant and dielectric permittivity of photosynthetic pigment–protein complexes noted in the preceding works

---

\* To whom correspondence should be addressed.

[11, 12]. The results of X-ray diffraction analysis of crystals of the protein complex of photosynthetic RC were from the Brookhaven Protein Databank (<http://www.rcsb.org/pdb>). Distances between centers of molecules were measured using the HyperChem 7 Professional software. The aggregate of the resulting estimates is the profile of distribution of effective dielectric constant along the electron transfer chain in the pigment–protein complex.

### BACTERIAL REACTION CENTERS AND PHOTOSYSTEM I

Although the PS I complex differs significantly from the RC of purple photosynthetic bacteria, there are features of remarkable similarity between PS I and BRC, especially in the RC core and the donor sites. The estimates of the effective dielectric constant values for the BRC of *Blastochloris* (formerly *Rhodopseudomonas*) *viridis* are given in Table 1. It was shown in our earlier studies that electrogenic reduction of the photooxidized bacteriochlorophyll dimer P960 by the immediate electron donor, high-potential cyt  $c_{559}$ , and further electron transfer from the second high-potential cyt  $c_{556}$  to oxidized cyt  $c_{559}$  account for 15 and 5% of the overall photoresponse amplitude  $\Delta\psi$ , respectively [13]. The same relative photovoltages and effective dielectric constant values were obtained for the donor sites of the *Rhodospirillum rubrum* and *Rhodobacter sphaeroides* BRC [14].

Comparison of the distance vector projections onto the membrane normal with the relative photovoltage amplitudes in PS I and BRC demonstrated that the  $\epsilon$  values corresponding to the electron transfer from the native donor proteins to P700 and P960 (or P870 in case of the other BRC species) were close to one another. Note that

the electron transport reactions at the donor side of PS I and BRC share the following features of similarity: (i) Gibbs energy difference ( $\Delta G$ ) between plastocyanin (Pc)/cyt  $c_6$  and P700 is close to  $\Delta G$  between cyt  $c_2$  and P870; (ii) electron transfer kinetics and proposed reaction mechanisms are very similar.

The main electrogenic step on the acceptor side of BRC is due to protonation of the doubly reduced secondary quinone  $Q_B$  [15]. The  $\epsilon$  value in this region is  $\sim 20$  [16], which is about 3 times higher than that at the acceptor region of PS I. Note also that the thermodynamic and kinetic properties of the terminal acceptors in two complexes significantly differ. The redox midpoint potential ( $E_m$ ) values of the  $Q_A/Q_A^-$  and  $Q_B/Q_B^-$  redox couples in BRC are in the range of  $-50$  to  $+100$  mV, whereas the  $E_m$  values of  $F_X$ ,  $F_A$ , and  $F_B$  in PS I are much more negative (range of  $-500$  to  $-700$  mV). The lifetimes of the electron and proton transfer reactions on the acceptor side of BRC (submillisecond time range) are at least three orders of magnitude lower than those values at the domain of the iron-sulfur clusters in PS I (range of tens- to hundreds of nanoseconds). Perhaps, the three-order-of-magnitude difference between the rate constants of charge transfer on the acceptor side of BRC and PS I, and threefold increase in the estimated value of  $\epsilon$  reflects the hypothetical correlation between the reaction rates and the dielectric properties of the corresponding protein domains between redox cofactors suggested in our earlier works [11, 12].

### PHOTOSYSTEM II

Recently determined crystal structures of PS II core complex from the cyanobacteria *Synechococcus elongatus*, *Thermosynechococcus vulcanus*, and *Thermosynechococcus elongatus* [17–19] were resolved at 3.8, 3.7, and 3.5 Å res-

**Table 1.** Calculation of effective dielectric constant values in the protein domains between redox cofactors in bacterial photosynthetic reaction centers of *Blastochloris viridis*

BRC protein domains between redox cofactors	Projections of the distance vectors ( $D$ ), Å*	Relative photovoltage ( $\psi$ ), relative units**	Effective dielectric constant value ( $\epsilon$ )
cyt $c_{556}$ – cyt $c_{559}$	24	0.05	34
cyt $c_{559}$ – P960	21	0.15	9.8
P960 – BPheo	15	0.35	3
BPheo – $Q_A$	15	0.35	3
$Q_B$ – protein/water boundary	39	0.1	27

\* The distances along the axis normal to the membrane plane are given according to the X-ray data [31].

\*\* Relative contributions of partial reactions to the overall electrogenesis were revealed in [13] and [32].

**Table 2.** Calculation of effective dielectric constant values in the protein domains between redox cofactors of PS II

PS II protein domains between redox cofactors	Projections of distance vectors ( $D$ ), Å*	Relative photovoltages ( $\psi$ ), relative units**	Effective dielectric constant values ( $\epsilon$ )
[Mn] <sub>4</sub> – Y <sub>Z</sub>	9.4	0.03	7.4
Y <sub>Z</sub> – P680	5.5	0.12	4.7
P680 – Pheo	12.3	0.43	3
Pheo – Q <sub>A</sub>	10	0.36	3
Q <sub>B</sub> – protein/water boundary	12	0.06	23

\* Distances along the axis normal to the membrane plane are given according to the atomic coordinates obtained from Protein Data Bank (Accession codes 1FE1 [17], 1IZL [18], and 1S5L [19]).

\*\* Relative contributions of partial reactions to the overall electrogenesis were revealed in [22, 25-29].

olution, respectively. It follows from these data that the arrangement of the electron transfer cofactors in PS II is rather similar to that in RCs of purple bacteria. The cofactors form two branches organized symmetrically along the pseudo-C2 axis connecting the P680 chlorophyll dimer center and nonheme iron atom. This symmetry is broken at the luminal side of D1 protein by the redox-active Tyr161 (Y<sub>Z</sub>) and the manganese cluster [Mn]<sub>4</sub>, which is located ~15 Å off the pseudo-C2 axis.

The kinetics and the quantum yield of the primary charge separation in pea chloroplasts were studied using the light-gradient technique [20, 21]. The charge separation occurred with two electrogenic phases: the faster phase with the rise-time <50 psec was ascribed to the electron transfer from the primary donor Chl (chlorophyll) dimer P680 to the intermediary acceptor pheophytin (Pheo), while the slower phase (~500 psec) was attributed to the electron transfer from Pheo to the primary quinone acceptor Q<sub>A</sub>. The relative photovoltage contributions of the faster and slower phases were approximately equal to each other. Fast photovoltage measurements using PS II membranes electrically oriented in a microcoaxial cell [22] and using PS II-containing proteoliposomes attached to a planar phospholipid membrane [6, 23, 24, 26-28] showed that electron transfer from Y<sub>Z</sub> to P680<sup>+</sup> spanned a dielectrically weighted distance of 13-18% of the distance between P680 and Q<sub>A</sub> [24, 25]. The dielectrically weighted distance of the electron transfer from [Mn]<sub>4</sub> to Y<sub>Z</sub><sup>ox</sup> (S<sub>1</sub>→S<sub>2</sub> transition of the oxygen-evolving complex) was estimated to be less than 3.5% [26, 27]. Larger electrogenic components (about 7%) were attributed to proton transfer from the oxidized cofactor X to the lumen phase during the transition S<sub>2</sub>→S<sub>3</sub> [26].

The charge transfer reaction associated with protonation of double-reduced secondary plastoquinone Q<sub>B</sub><sup>2-</sup> at the acceptor side contributes about 5% to the overall electrogenesis in PS II [23, 24]. However, it should be noted that this estimate most probably represents the lower limit

of the relative contribution of this reaction, because: (i) there were some indications that the reconstruction of the Q<sub>B</sub> function in the PS II particles used in these experiments was incomplete and (ii) slow component of  $\Delta\psi$  decay (characteristic of the oxygen-evolving complex activity [29]) contributed only ~50% to the overall laser flash-induced  $\Delta\psi$  decay [23]. It was shown recently in our laboratory using PS II preparations, in which the contribution of the slow component of the  $\Delta\psi$  decay reached ~90%, the amplitude of the electrogenic phase attributed to Q<sub>B</sub><sup>2-</sup> protonation was ~11% of total amplitude of  $\Delta\psi$  [28]. The distance between the Q<sub>B</sub>-binding site and protein globule boundary in PS II complexes is smaller than in BRC [19]. Therefore, it is safe to suggest that the dielectric properties in the Q<sub>B</sub>-protein boundary domain of PS II are similar to that of BRC (Tables 1 and 2).

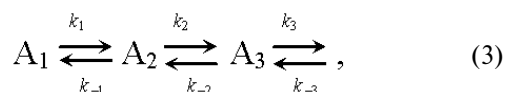
The data shown in Table 2 give the results of comparison of the distance vectors between the redox cofactors in PS II with relative photovoltages accompanying corresponding charge transfer reactions. Like in the case of the BRC (see Table 1), the  $\epsilon$  value in the protein domain between the Chl (bacteriochlorophyll) dimer and Q<sub>A</sub> is the lowest, whereas it gradually increases at the donor side. A similar increase in the effective dielectric constant is observed at the donor side of PS I [11, 12]. Note that the  $\epsilon$  value in the domain between Y<sub>Z</sub> and P680 is only ~1.5 times higher than that at the P680–Q<sub>A</sub> region, while the  $\epsilon$  values in the Pc–P700 and cyt c<sub>559</sub>–P960 protein regions of PS I and BRC, respectively, increase about threefold relative to the hydrophobic core domains (Tables 1 and 2), which is seemingly consistent with higher electron transfer rate (30 nsec [22]) compared to that at the donor sides of PS I and BRC (microsecond-to-millisecond lifetime range). On the other hand, the values of  $\epsilon$  calculated for the [Mn]<sub>4</sub>–Y<sub>Z</sub>, Pc–P700, and cyt c<sub>559</sub>–P960 protein regions were larger than that for Y<sub>Z</sub>–P680, and comparable with each other, which seems to be consistent with similar rate constants of corresponding electron transfer reactions.

Because similar patterns of distribution of dielectric constant are observed at least in three photosynthetic systems with different structures, it is safe to suggest that such a character of dielectric constant distribution is a general property inherent in photosynthetic charge transfer processes rather than a unique characteristic of specific pigment–protein complexes.

#### POSSIBLE MECHANISM OF CORRELATION BETWEEN KINETIC, THERMODYNAMIC, AND DIELECTRIC PROPERTIES OF REACTION CENTERS

The process of charge transfer in biological systems proceeds through several stages including tunneling and further stabilization of energy levels. The efficiency of the process substantially depends on the dielectric reorganization of medium. Effective processes of relaxation (e.g., polarization) in the locus of reaction groups are required to provide stabilization of separated charges. Perhaps, the above-mentioned correlation between the rate constant of charge transfer reaction and dielectric constant in PS I complex is due to relaxation processes.

Let us consider the process of electron transfer along the chain composed of a series of several carriers  $A_1$ ,  $A_2$ ,  $A_3$ , etc.:



where  $k_1$  and  $k_{-1}$  are the rate constants of direct and back transfer at the segment  $A_1 \rightleftharpoons A_2$ , respectively.

The concentration changes of the carrier  $A_1$  contain kinetic components corresponding to both direct and back reactions ( $k_1$  and  $k_{-1}$ ). However, the amplitude contribution of the kinetic component corresponding to back reaction ( $k_{-1}$ ) is determined by the ratio of the rates of direct and back transfer  $A_2$  ( $k_2$  and  $k_{-1}$ ). For example, if  $k_2 \gg k_{-1}$ , an electron from  $A_2$  is rapidly transferred to  $A_3$ , and the amplitude contribution of the kinetic component corresponding to the rate constant of back transfer ( $k_{-1}$ ) is small. The total rate of concentration changes of carrier  $A_1$  in this case is determined by the rate constant  $k_1$  of fast direct reaction. Otherwise, ( $k_2 \sim k_{-1}$ ), the total rate of concentration changes of carrier  $A_1$  is slowed down. The negative logarithm of the rate constant of the back reaction is proportional to activation ( $\Delta G$ ). At large value of  $\Delta G$ , the probability of back transfer is low, whereas this probability increases upon decreasing the  $\Delta G$ . The reaction becomes substantially reversible and the total rate of the process decreases.

The primary processes of electron transfer in photosynthesis are characterized by high rates (reaction time, from pico- to nanoseconds) and large value of  $\Delta G$  (up to

0.3 eV). As the electron goes farther from the primary pair of chlorophyll molecules, the value of  $\Delta G$  decreases and reaction time increases. Perhaps, such energy “exchange” for reaction time is of functional significance. High rate and large  $\Delta G$  of primary reactions increase the quantum yield of photosynthesis (up to ~100%) and prevent functionally useless recombination of separated charges. On the other hand, small value of  $\Delta G$  and relatively large reaction time at the peripheral segments of chain provide more effective coupling of electron transfer with metabolic and energy storage reactions (e.g., accumulation of reduced products).

Ionizable amino acid residues and free water molecules in the vicinity of electron-transport cofactors give rise to appearance of polarization sublevels, decrease in the value of  $\Delta G$ , and increase in the dielectric constant  $\epsilon$ . Let us consider the distribution of ionizable amino acid residues and free water molecules in the vicinity of electron-transport cofactors at the acceptor side of PS I by the example of the iron-sulfur centers  $F_X$ ,  $F_A$ , and  $F_B$  (Table 3).

In the preceding works we obtained the following estimates of  $\epsilon$  distribution along the electron transfer chain in the pigment–protein complexes of PS I:  $\epsilon \sim 5.4$  ( $A_0 \rightarrow A_1$  and  $A_1 \rightarrow F_X$ ),  $\epsilon \sim 8.7$  ( $F_X \rightarrow F_A$ ), and  $\epsilon \sim 4.6$  ( $F_A \rightarrow F_B$ ) [11, 12]. These estimates of  $\epsilon$  are qualitatively consistent with the pattern of distribution of water molecules and ionizable amino acid residues (Asp, Glu, Lys, Arg, and His) in the loci of the electron transfer chain. The numbers of ionizable amino acid residues in the vicinity of the iron-sulfur clusters  $F_X$ ,  $F_A$ , and  $F_B$  (at distances  $< 11$  Å from each cluster), determined from the X-ray diffraction analysis of the PS I protein crystals, are 13, 15, and 3, respectively. With regard to the effect of compensation of closely located opposite charges (distance  $< 3.5$  Å) [30], these numbers are 5, 9, and 3, respectively. Although the general trend toward an increase in the value of  $\epsilon$  along the direction from the primary pair to the periphery of the complex is valid in this case too, there is a deviation from this trend at the site  $F_A \rightarrow F_B$ , where distribution of water molecules and polar amino acid residues is abnormal. The cause of the anomaly is presently obscure.

Thus, BRC complexes are similar to PS I and PS II complexes not only in terms of hierarchy of electron transfer rate constants and energy gaps between neighboring carriers but also in terms of hierarchy of distribution of local effective dielectric constant. Possible mechanisms of correlation between these parameters deserve more profound experimental and theoretical research.

This study was supported by Grant from the International Science and Technology Center (ISTC) 2296 (to A. Y. S.), Grant 01-483 from the INTAS (to A. Y. S.), Grants from the Russian Foundation for Basic Research 03-04-49219 (to S. K. C.) and 03-04-48983 (to

**Table 3.** Distances (*D*) from iron-sulfur centers to closest polar amino acid residues and water molecules in PS I complexes

Iron-sulfur centers	Amino acid residues										Water				
	ASP		GLU		LYS		ARG		HIS		Total ( <i>D</i> <11 Å)	Total ( <i>D</i> <11 Å) with regard to compen- sation	No.	<i>D</i> , Å	Total
	No.	<i>D</i> , Å	No.	<i>D</i> , Å	No.	<i>D</i> , Å	No.	<i>D</i> , Å	No.	<i>D</i> , Å					
1	2	3	4	5	6	7	8	9	10	11	12	13	14	15	16
<b>F<sub>x</sub></b>	575	6.6	54 <sup>b</sup>	10.8	51 <sup>b</sup>	9.0	728 <sup>d</sup>	5.1			<b>13</b>	<b>5</b>	162	4.2	<b>20</b>
	579 <sup>a</sup>	8.3	62 <sup>a</sup>	14.2			712 <sup>c</sup>	5.6					43	5.3	
	566 <sup>b</sup>	8.6					694	9.4					12	5.3	
	593 <sup>d</sup>	8.6					674	9.6					190	6.0	
	580 <sup>c</sup>	9.2					583 <sup>a</sup>	9.7					73	6.3	
	568 <sup>a</sup>	14.2					570 <sup>b</sup>	10.5					37	6.4	
							65 <sup>b</sup>	11.2					67	6.4	
							52 <sup>a</sup>	12.0					6	6.6	
													26	6.9	
													145	7.0	
													36	7.0	
													56	7.4	
													132	8.1	
										64	8.3				
										76	8.4				
										160	8.4				
										159	8.5				
										188	8.7				
										158	8.9				
										157	9.2				

Table 3 (Contd.)

1	2	3	4	5	6	7	8	9	10	11	12	13	14	15	16
<b>F<sub>A</sub></b>	579 <sup>a</sup>	7.3	54 <sup>b</sup>	7.3	51 <sup>b</sup>	8.4	583 <sup>a</sup>	6.9	2	7.0	15	9	167	6.5	11
	23	8.3	62 <sup>a</sup>	8.1	5	8.9	52 <sup>a</sup>	7.7					25	6.6	
	46 <sup>c</sup>	9.6	45	10.7			60	9.6					6.6	6.8	
	568 <sup>a</sup>	11.3	71	10.7			43	9.9					145	6.8	
	566 <sup>b</sup>	11.4					65 <sup>b</sup>	10.2					76	8.0	
<b>F<sub>B</sub></b>							570 <sup>b</sup>	12.0					89	8.4	
							74 <sup>c</sup>	12.6					165	8.4	
													166	8.6	
													34	8.8	
													119	9.4	
													120	10.4	
	8	10.4	54 <sup>b</sup>	10.1	51 <sup>b</sup>	13.2	18	9.4			3	3	182	6.9	8
	566 <sup>b</sup>	13.4					65 <sup>b</sup>	11.4					126	7.1	
							570 <sup>b</sup>	11.7					183	7.6	
													82	7.8	
													184	9.0	
													81	9.5	
													167	10.0	
													148	10.6	

Note: The structure file was taken from RCSB Protein Data Bank, PDB ID: 1JB0 [25]. Distance measurements were performed using VMD 1.7.1 software (Theoretical Biophysics Group, Beckman Institute for Advanced Science and Technology, University of Illinois). Distance *D* from amino acid residue to iron-sulfur center was measured as the shortest distance between the charged residue and the closest iron atom of the center. Groups of residues compensating each other are denoted as:

<sup>a</sup> ASP579, ASP568, GLU62, ARG583, ARG52; net charge –1;

<sup>b</sup> ASP566, GLU54, LYS51, ARG570, ARG65; net charge +1;

<sup>c</sup> ASP580, ARG712; net charge 0;

<sup>d</sup> ASP593, ARG728; net charge 0;

<sup>e</sup> ASP46, ARG74; net charge 0.

A. Y. S.), and Grant RC1-2400-MO-02 (to A. Y. S.) from the Civilian Research and Development Foundation (CRDF).

## REFERENCES

- Drachev, L. A., Jasaitis, A. A., Kaulen, A. D., Kondrashin, A. A., Liberman, E. A., Nemecek, I. B., Ostroumov, S. A., Semenov, A. Yu., and Skulachev, V. P. (1974) *Nature*, **249**, 321-324.
- Drachev, L. A., Kaulen, A. D., Khitrina, L. V., and Skulachev, V. P. (1981) *Eur. J. Biochem.*, **117**, 461-470.
- Drachev, L. A., Semenov, A. Yu., Skulachev, V. P., Smirnova, I. A., Chamorovsky, S. K., Kononenko, A. A., Rubin, A. B., and Uspenskaya, N. Ya. (1981) *Eur. J. Biochem.*, **117**, 483-489.
- Mamedov, M. D., Gadjeva, R. M., Gourovskaya, K. N., Drachev, L. A., and Semenov, A. Yu. (1996) *J. Bioenerg. Biomembr.*, **28**, 517-522.
- Vassiliev, I. R., Jung, Y.-S., Mamedov, M. D., Semenov, A. Yu., and Golbeck, J. H. (1997) *Biophys. J.*, **72**, 301-315.
- Mamedov, M. D., Lovyagina, E. R., Verkhovsky, M. I., Semenov, A. Yu., Cherepanov, D. A., and Shinkarev, V. P. (1994) *Biochemistry (Moscow)*, **59**, 685-690.
- Lockhart, D. J., and Kim, P. S. (1992) *Science*, **257**, 947-951.
- Steffen, M. A., Lao, K., and Boxer, S. G. (1994) *Science*, **264**, 810-816.
- Finkel'shtein, A. V., and Ptitsyn, O. B. (2002) *Protein Physics* [in Russian], Knizhnyi Dom Universitet, Moscow.
- Fersht, A. (1999) *Structure and Mechanism in Protein Science: A Guide to Enzyme Catalysis and Protein Folding*, Freeman, New York.
- Semenov, A. Yu., Mamedov, M. D., and Chamorovsky, S. K. (2003) *FEBS Lett.*, **553**, 223-228.
- Semenov, A. Yu., Chamorovsky, S. K., and Mamedov, M. D. (2004) *Biofizika*, **49**, 227-238.
- Dracheva, S. M., Drachev, L. A., Konstantinov, A. A., Semenov, A. Yu., Skulachev, V. P., Arutyunian, A. M., Shuvalov, V. A., and Zaberezhnaya, S. M. (1988) *Eur. J. Biochem.*, **171**, 253-264.
- Semenov, A. Yu. (1991) *Electrogenic Reactions in Photosynthetic Reaction Centers of Purple Bacteria*, in *Soviet Scientific Reviews/Section D* (Skulachev, V. P., ed.) Vol. 10, pp. 45-75, Harwood Academic Publishers, UK.
- Kaminskaya, O. P., Drachev, L. A., Konstantinov, A. A., Semenov, A. Yu., and Skulachev, V. P. (1986) *FEBS Lett.*, **2**, 224-228.
- Shinkarev, V. P., Drachev, L. A., Mamedov, M. D., Mulkidjanian, A. Ya., Semenov, A. Yu., and Verkhovsky, M. I. (1993) *Biochim. Biophys. Acta*, **1144**, 285-294.
- Zouni, A., Witt, H.-T., Kern, J., Fromme, P., Krauss, N., Saenger, W., and Orth, P. (2001) *Nature*, **409**, 739-743.
- Kamiya, N., and Shen, J.-R. (2003) *Proc. Natl. Acad. Sci. USA*, **100**, 98-103.
- Ferreira, K. N., Iverson, T. M., Maghlaoui, K., Barber, J., and Iwata, S. (2004) *Science*, **303**, 1831-1838.
- Trissl, H.-W., and Leibl, W. (1989) *FEBS Lett.*, **244**, 85-88.
- Leibl, W., Breton, J., Deprez, J., and Trissl, H.-W. (1989) *Photosynth. Res.*, **22**, 257-275.
- Pokorny, A., Wulf, K., and Trissl, H.-W. (1994) *Biochim. Biophys. Acta*, **1184**, 65-70.
- Mamedov, M. D., Beshta, O. E., Samuilov, V. D., and Semenov, A. Yu. (1994) *FEBS Lett.*, **350**, 96-98.
- Hook, F., and Brzezinski, P. (1994) *Biophys. J.*, **66**, 2066-2072.
- Jordan, P., Fromme, P., Klukas, O., Witt, H. T., Saenger, W., and Krauss, N. (2001) *Nature*, **411**, 909-917.
- Haumann, M., Mulkidjanian, A., and Junge, W. (1997) *Biochemistry*, **36**, 9304-9315.
- Mamedov, M. D., Beshta, O. E., Gourovskaya, K. N., Mamedova, A. A., Neverov, K. D., Samuilov, V. D., and Semenov, A. Yu. (1999) *Biochemistry (Moscow)*, **64**, 504-509.
- Mamedov, M. D., Tyunyatkina, A. A., and Semenov, A. Yu. (2005) *Biochemistry (Moscow)*, in press.
- Rutherford, W., and Boussac, A. (1992) in *Research in Photosynthesis. Proc. 9th Int. Congr. on Photosynthesis* (Murata, N., ed.), Vol. 2, pp. 21-27, Kluwer Academic Publishers, Dordrecht, The Netherlands.
- Antonkine, M. L., Jordan, P., Fromme, P., Krauss, N., Golbeck, J. H., and Stehlik, D. (2003) *J. Mol. Biol.*, **327**, 671-697.
- Deisenhofer, J., Epp, O., Miki, K., Huber, R., and Michel, H. (1984) *Nature*, **318**, 618-624.
- Deprez, J., Trissl, H. W., and Breton, J. (1986) *Proc. Natl. Acad. Sci. USA*, **83**, 1699-1703.